Electric Vehicle-to-Vehicle Energy Transfer Using On-Board Converters

Azizulrahman Shafiqurrahman, *Student Member, IEEE*, B. S. Umesh, *Member, IEEE*, Naji Al Sayari, *Member, IEEE*, and Vinod Khadkikar, *Fellow, IEEE*

***Abstract*— Electric vehicle-to-vehicle (V2V) charging is a recent approach for sharing energy among electric vehicles (EVs). Existing V2V approaches with an off-board power-sharing interface add extra space and cost for EV users. Furthermore, V2V power transfer using on-board type-2 chargers reported in the literature is not efficient due to redundant conversion stages. This article proposes a new method for V2V power transfer by directly connecting the two EV batteries together for sharing energy through the type-2 ac charger input ports and switches. The active rectifiers of on-board type-2 chargers are not used for rectification during V2V charging, instead only a few switches are used as interfaces to connect the two EV batteries together, to avoid redundant power conversion and associated losses which effectively improve the overall V2V efficiency. The possible V2V charging scenarios of the proposed V2V approach are validated using a MATLAB/Simulink simulation study. Furthermore, a scaled experimental prototype is developed to validate the proposed V2V method practically.**

***Index Terms*— Electric vehicle (EV), on-board type-2 ac charger, vehicle-to-vehicle (V2V) charging.**

I. Introduction

THE electric vehicle (EV) charging is conventionally done through type-1 and -2 (single/three-phase) ac on-board slow chargers with the power range of 3.3–19.4 kW. A comprehensive review of bidirectional topologies with single/two-stage rectification with power factor correction for on-board chargers in the commercial EVs is discussed in [1] and [2]. Detailed comparison of type-1, -2, and the dc fast-charging stations with respect to charging time, power density, power level, cost, and review of recent typologies for conventional and future charging methods is discussed in [3] and [4]. Furthermore, high power (>50 kW) external off-board dc fast-charging stations are established to charge EV batteries, with a charging time of less than an hour [5]. In spite of these conventional EV charging methods, the EV users are experiencing range anxiety due to limited charging infrastructure [6].

In recent days, vehicle-to-vehicle (V2V) charging is emerging as an alternate method to share energy between two EVs, in the case of nonavailability of both the ac grid and the dc fast-charging stations. The V2V charging allows EV users to cooperatively share energy with each other with minimum infrastructure and cost and reduce range anxiety. Mainly there are two aspects to V2V energy sharing: first, the communication aspects of V2V, which provides a platform for EV users to interact with each other to find the energy sharing match, to decide provider and receiver preferences, and tariff. In [7]–[10] game theory-based algorithms to match the receiver EV, provider EV, the nearest meeting point, and the communication aspects of the V2V are presented.

The second important aspect of V2V is the power interface for the actual power transfer, that is, controlling the direction of power flow based on the receiver and provider preference, and a buck or boost conversion based on the EV battery's voltage level. Using the ac power grid as a common energy aggregator with off-board bidirectional power converters for accomplishing an indirect V2V energy transfer is one of the basic V2V approaches presented in [11] and [12] where the conversion efficiency is low due to multiple redundant conversion stages. An off-board V2V charger using an off-board bidirectional interleaved dc–dc converter with a possibility of integration to the grid is presented in [13]. Similar V2V charging approaches with an off-board power interface are presented in [14] and [15].

Similarly, a commercial 50 kW off-board V2V charger from Andromeda Power is available in the market to share energy between two EVs [16], [17]. But this off-board V2V approach requires an external V2V interface which may result in extra cost and car space for the EV users.

On the other hand, V2V approaches by re-utilizing the on-board type-1 and -2 chargers as power interfaces are presented in [18] and [19]. Basically, the on-board type-1 and -2 chargers consist of an ac to dc converter (active rectifier) stage followed by a dc–dc converter [for constant current and constant voltage (CCCV) charge control]. In [18], a V2V charging approach by connecting the type-1 charger input ports of the two EVs is presented as shown in Fig. 1(a), wherein the provider EV battery dc output is first converted into single-phase ac using the bidirectional two-stage on-board type-1 ac charger. This ac power output of the provider EV is fed as input to the two-stage on-board type-1 converter to charge the receiver EV battery. Cascaded converter losses due to redundant conversion stages lead to lower V2V charging efficiency in [18]. In [19], V2V charging by directly

Manuscript received 8 January 2022; revised 1 April 2022; accepted 15 April 2022. Date of publication 2 May 2022; date of current version 21 February 2023. This work was supported by the Advanced Power and Energy Centre (APEC), Khalifa University, Abu Dhabi, United Arab Emirates. *(Corresponding author: Vinod Khadkikar.)*

The authors are with the Advanced Power and Energy Centre (APEC), Department of Electrical Engineering and Computer Science, Khalifa University, Abu Dhabi, United Arab Emirates (e-mail: 100058331@ku.ac.ae; umesh.baktharahalli@ku.ac.ae; naji.alsayari@ku.ac.ae; vinod.khadkikar@ku.ac.ae).

Digital Object Identifier 10.1109/TTE.2022.3172029

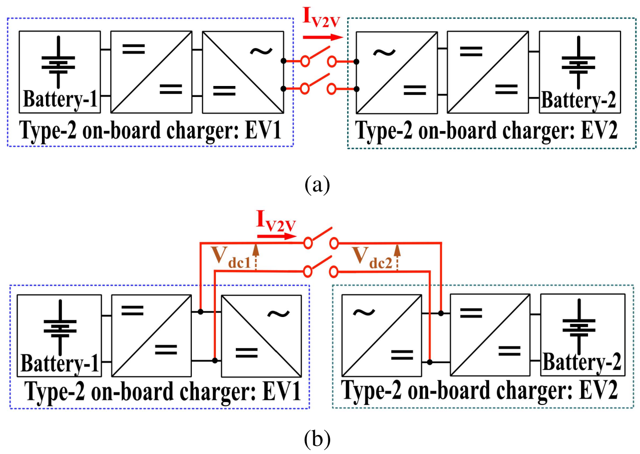

Fig. 1. V2V operations: (a) ac V2V operation and (b) dc V2V operation.

connecting the dc-link of the two EVs using mechanical switches is presented as shown in Fig. 1(b). However, practically, there is no direct access to the dc-link of battery side dc–dc converters for establishing the presented direct connection. Thus, the V2V approach presented in [19] is not a practically feasible solution without customized design modifications and additional charging ports for bringing out the dc-link terminals of the two EVs.

This article proposes a V2V charging approach for EVs through the on-board type-2 chargers by directly connecting the on-board type-2 power inlet ports, which eliminates the need for external hardware or additional power inlet ports for V2V operation. Furthermore, the proposed V2V approach utilizes the active rectifier stages as a connection interface to connect two EV batteries which in turn reduces the total conversion stages in the V2V energy transfer path. Reduced conversion stages reduce the overall active switches contributing to switching and conduction losses which significantly increases the efficiency. In the proposed V2V approach, mode selection logic is presented to decide buck/boost operating modes, based on the battery voltage levels and the power flow direction, based on the EV user's preference. Control of power flow in either direction provides greater flexibility for the EV users to be a provider or receiver irrespective of the difference in both EV battery voltage ratings. The proposed approach of connecting the two EV batteries through on-board active rectifier switches eliminates the need for an off-board V2V interface unlike [16], additional contactor switches in contrast to [19], redundant power transfer stages compared to [18], and associated losses that improve the overall V2V efficiency.

The rest of the article is structured as follows. In Section II, the power converter configuration and its operating modes for possible V2V modes of the proposed approach are discussed. The control scheme for the proposed V2V approach is described in Section III. Performance improvement of the proposed V2V with respect to efficiency and other aspects are discussed in detail in Section IV in addition to simulation results. The experimental validation of the proposed V2V approach with a scaled lab prototype is discussed in Section V. Finally, the article is concluded in Section VI.

II. Proposed V2V Approach

The proposed V2V configuration is realized by connecting the existing type-2 charging ports of the provider-EV and the receiver-EV. The two EVs are connected by utilizing the three-phase active rectifier switches. Turning ON the top switch of one of the phases (phase-a, S_1 here) and bottom switch of the other phase (phase-c, S_6 here) of the active rectifier-1 and the respective phase switches S_1' and S_6' of the active rectifier-2 directly connects the two EV batteries through the intermediate dc-link of provider and receiver EVs as shown in Fig. 2. The four switches S_1, S_6, S_1', and S_6' are kept ON throughout the V2V power transfer duration. The proposed way of connecting the two EVs realizes a dual bidirectional buck-boost converter that can be controlled to transfer energy between two EVs in either direction regardless of their battery voltage levels.

As the active rectifiers of both the type-2 chargers are used as an interface to connect two dc-links instead of their actual purpose of rectification, other switches of both the active rectifiers are kept OFF throughout the V2V operation. Based on the battery voltage of two EVs, the configuration may operate in one of the possible energy transfer modes as discussed below.

A. V2V Scenario-1: $V_{bat1} < V_{bat2}$

With the EV-1 battery voltage less than the EV-2 battery voltage and provider–receiver role, there are two possible scenarios of boost and buck operation with power flow in forward or reverse direction, respectively, as explained below.

1) Forward Boost Mode (EV1 as Provider and EV2 as Receiver): In this mode, EV1 is charge provider and EV2 is charge receiver with battery-1 having lower voltage than battery-2. Once the direct connection of two EV batteries through the proposed approach (by turning on the switches S_1, S_6, S_1', and S_6'), EV-1 battery voltage is stepped up to the EV-2 battery voltage by operating the dc–dc converter-1 in the boost mode. During the turn ON period of the switch S_{b1}, inductor L_1 stores energy from EV-1 battery, and the switch S_{a1} is complimentary switched to S_{b1} as shown in Fig. 3(a). When S_{b1} is turned OFF, S_{a1} gets turned ON to transfer energy of EV-1 battery and inductor L_1 to EV-2 battery through S_1, S_1', S_{a2}, and inductor L_2. To receive power from the dc-links, switch $Sa2$ is kept on throughout this V2V mode which makes $V_{dc1} = V_{dc2} = V_{bat2}$ and switch S_{b2} is complimentary switched to S_{a2} as shown in Fig. 3(b).

2) Reverse Buck Mode (EV1 as Receiver and EV2 as Provider): Similar to the forward boost mode in this reverse buck mode, the EV batteries are connected by turning on the switches S_1, S_6, S_1', and S_6' of the active rectifier-1 and 2. The dc–dc converter-1 is operated in buck mode to transfer power from EV-2 battery to EV-1 battery. The diode D_{a2} gets forward biased as $V_{bat1} < V_{bat2}$ leading to $V_{bat2} = V_{dc1} = V_{dc2}$ and thus making EV-2 battery available for delivering power to EV-1 battery through the dc-link. During turn ON period of switch S_{a1}, the energy from the EV-2 battery is transferred to EV-1 battery through inductor L_1, D_{a2}, S_1', and inductor L_2 as shown in Fig. 4(a). During the turn OFF period of S_{a1}, the

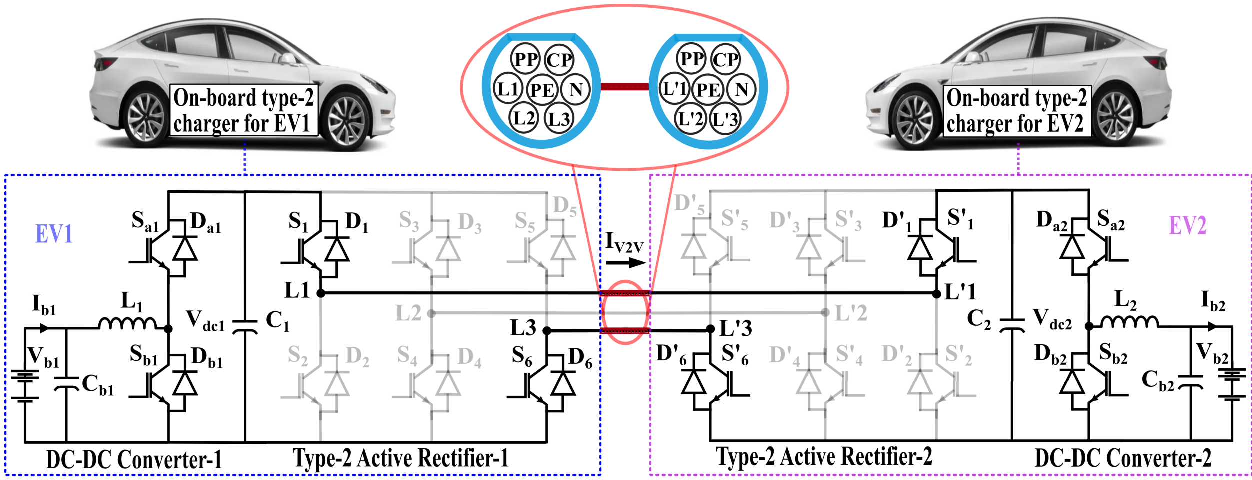

Fig. 2. Proposed topology for V2V operation.

energy in the inductor L_1 freewheel through switch S_{b1} which is complementary switched to S_{a1} as shown in Fig. 4(b).

B. V2V Scenario-2: $V_{bat1} = V_{bat2}$

In this scenario as both EV battery voltages are equal, the dc–dc converters need to be controlled, one in current-controlled boost mode and the other in current-controlled buck mode.

1) Forward Boost Mode (EV1 as Provider and EV2 as Receiver): In this mode with $V_{\text{bat1}} = V_{\text{bat2}}$, power transfer from EV-1 to EV-2 battery is achieved by operating the dc–dc converter-1 in the boost mode and the dc–dc converter-2 is operated in the buck mode with closed-loop current control. During turn ON period of the switch S_{b1}, inductor L_1 stores energy from EV-1 battery and switch S_{a1} is complimentary switched to S_{b1}. At the same instant, the switch S_{b2} of dc–dc converter-2 is also ON to freewheel the energy in inductor L_2, and the switch S_{a2} is complimentary switched to S_{b2} as shown in Fig. 5(a). During the turn OFF period of S_{b1} and S_{b2}, the switches S_{a1} and S_{a2} gets turned on to transfer energy from EV-1 battery to EV-2 battery through L_1, S_1, S_1', and L_2 as shown in Fig. 5(b). This mode can also be achieved by operating provider EV side dc–dc converter in the voltage control mode to regulate the dc-link voltage at a higher voltage than the EV battery voltage and receiver-side dc–dc converter in the current control mode.

2) Reverse Boost Mode (EV1 as Receiver and EV2 as Provider): This mode is similar to the forward boost mode with $V_{\text{bat1}} = V_{\text{bat2}}$ but the power flow is reversed by operating the dc–dc converter-2 in boost mode and the dc–dc converter-1 is operated in buck mode with closed-loop current control. Voltage control mode could be used to control the power flow in this mode as well.

C. V2V Scenario-3: $V_{bat1} > V_{bat2}$

The converter operation in this scenario is similar to the Scenario-1 with the power flow direction reversed.

1) Reverse Boost Mode (EV1 as Receiver and EV2 as Provider): This mode is similar to the forward boost mode with $V_{\text{bat1}} < V_{\text{bat2}}$ but the power flow is reversed by operating the dc–dc converter-2 of EV-2 in the boost mode, and keeping the S_{a1} of the dc–dc converter-1 of EV-1 always ON.

2) Forward Buck Mode (EV1 as Provider and EV2 as Receiver): This mode is similar to the reverse buck mode with $V_{\text{bat1}} < V_{\text{bat2}}$ but the power flow is reversed by operating the dc–dc converter-2 of EV-2 in the buck mode, and keeping the S_{a1} of the dc–dc converter-1 of EV-1 always ON.

III. Control Scheme for the Proposed V2V Approach

The charging rate and the amount of energy transferred during the proposed V2V approach are controlled by controlling the on-board converters. The mode selector flow shown in Fig. 6 decides the V2V mode based on the EV-1 and EV-2 battery values and the provider receiver information. Furthermore, depending on the mode of operation, the on-board charger converters are controlled for achieving the proposed V2V as discussed next in this section.

A. Control of the Active Rectifiers as V2V Interface

Typically, during the normal three-phase ac charging through a type-2 charger, the active rectifier is controlled in d-q control mode to convert the three-phase ac to dc with unity power factor operation at the grid terminals. During the proposed V2V charging, the active rectifier is re-utilized as an interface to access and connect the batteries of the two EVs. After the type-2 charger ports are connected for V2V charging, the gating pulse for the switches S_1 and S_6 of the active rectifier-1 of the EV-1 and the switches S_1' and S_6' of the active rectifier-2 are kept active high throughout the V2V charging for all the modes.

B. Control of DC–DC Converters

For the proposed V2V charging approach using the on-board chargers, the dc–dc converters of the type-2 chargers are closed-loop current-controlled.

For forward boost and reverse buck mode control ($V_{\text{bat1}} < V_{\text{bat2}}$): In these modes, the dc–dc converter-1's inductor current I_{L1} in forward or reverse direction is controlled in

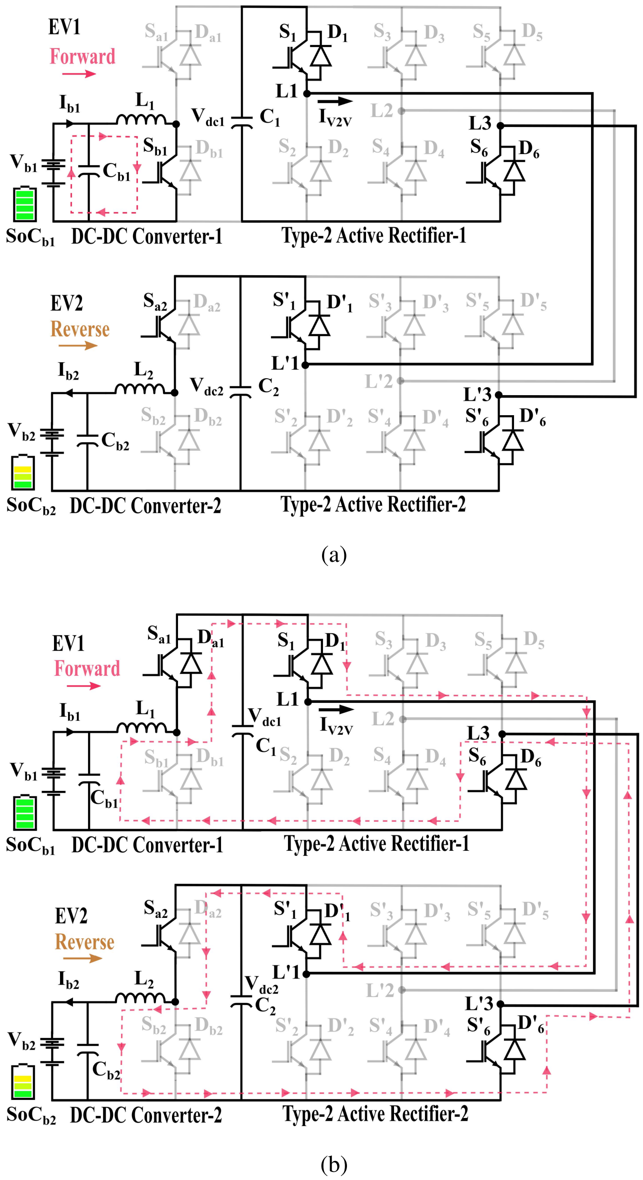

Fig. 3. Forward boost V2V mode with $V_{\text{bat1}} < V_{\text{bat2}}$. (a) L1 stores energy from EV-1 battery. (b) Energy is transferred through dc-link to EV2.

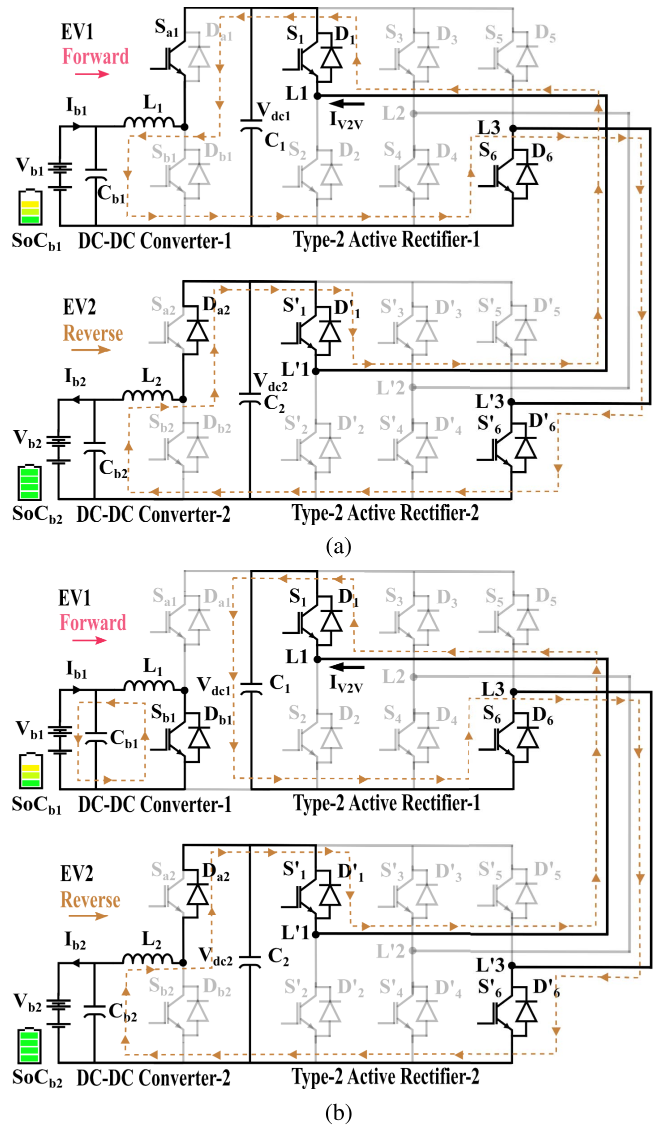

Fig. 4. Reverse buck V2V mode with $V_{\text{bat1}} < V_{\text{bat2}}$. (a) L1 stores energy from EV-2 battery through dc-link. (b) Energy is stored from L1 to EV-1 battery through freewheeling.

closed-loop by feeding the error between the reference current I_L^* and the actual inductor current I_{L1} to a PI controller to generate duty ratio for switch S_{a1}, and S_{b1} is complimentarily switched to S_{a1} as shown in Fig. 7. Gating signal to the switch S_{a2} is kept active high throughout this mode. The current to control transfer function to the dc–dc converter-1 used to tune the PI controller is given in the following equation, where D is the duty ratio and R_2 is the load resistance equivalent to charging current of the EV-2 battery [20]

$$\frac{\widehat{I_{L1}}(s)}{\widehat{d}(s)} = \frac{(C_1 V_{b1})s + 2(1-D)L_1}{(L_1 C_1)s^2 + \frac{L_1}{R_2}s + (1-D)^2}. \tag{1}$$

Reference current I_L^* is calculated based on the following equation, where E_{bat1} and E_{bat2} are kWh ratings of the EV-1 and EV-2 batteries, respectively, and T_c is the desired charging time. The minimum values among the two battery ratings and voltage levels are selected to calculate the reference current

$$I_L^* = \frac{\min(E_{\text{bat1}}, E_{\text{bat2}})}{\min(V_{\text{bat1}}, V_{\text{bat2}}) * T_c}. \tag{2}$$

The maximum value of I_L^* depends on current rating I_{s1r} of the on-board active rectifier IGBTs (S_1, S_6, S_1', and S_6'), if I_L^* computed from (2) exceeds I_{s1r}, the current reference will be caped to I_{s1r}. Similarly, for the forward buck and reverse boost mode with ($V_{\text{bat1}} > V_{\text{bat2}}$), the same control structure is used to control the I_{L2} in the forward or reverse direction by generating the duty ratio for the switch S_{b2} and switch S_{a2} is complimentarily switched to S_{b2}. The gating signal to switch S_{a1} is made active high throughout this mode.

Furthermore, in the forward boost mode with ($V_{\text{bat1}} = V_{\text{bat2}}$), both the dc–dc converters are operated in current control mode to control I_{L1} and I_{L2} in the forward direction. As both the battery voltages are equal in this case, the current reference

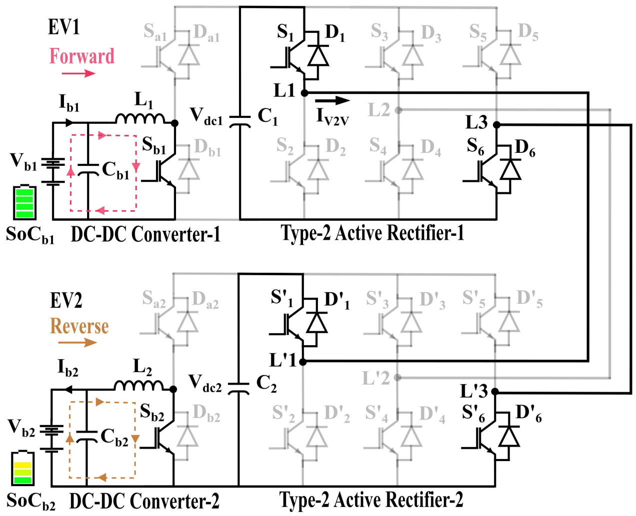

(a)

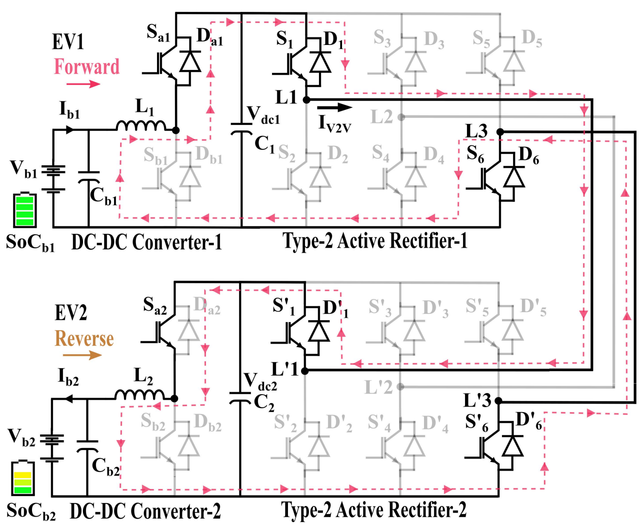

(b)

Fig. 5. Forward boost V2V mode with $V_{\text{bat1}} = V_{\text{bat2}}$. (a) L_1 and L_2 store energy from the batteries. (b) Energy is transferred through dc-link to EV2.

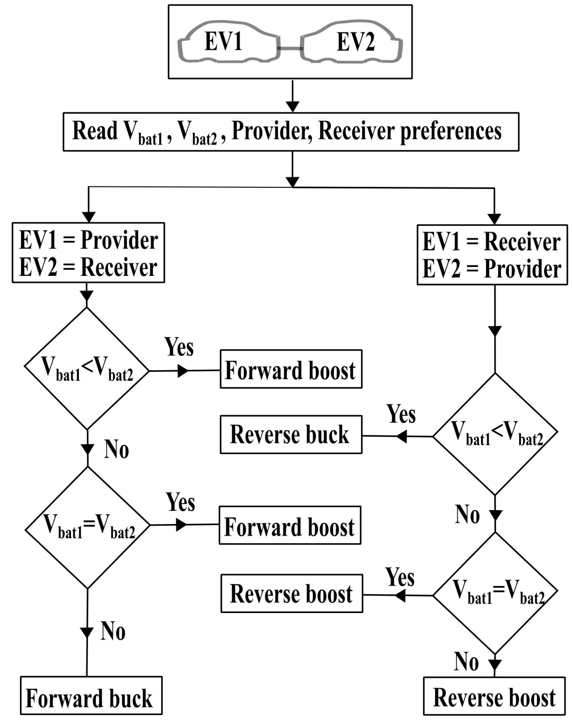

Fig. 6. Proposed V2V power transfer control flow.

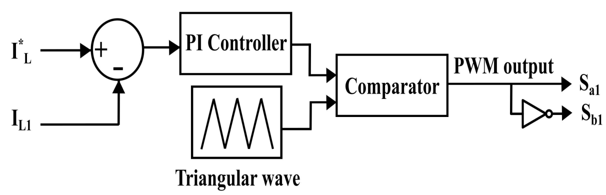

Fig. 7. Current control structure in forward boost and reverse buck modes ($V_{\text{bat1}} < V_{\text{bat2}}$).

I_L^* should be equal for both the dc–dc converters to maintain power balance at the two EV batteries. This mode can be controlled alternatively by regulating the dc-link at a higher voltage by operating one of the dc–dc converter-1 in voltage-controlled boost mode and the dc–dc converter-2 in current-controlled buck mode.

The higher efficiency, lower losses, and convenience of connecting two EVs through the existing on-board type-2 charger ports make the proposed V2V approach more practically adaptable among EV users. In general, for the practical implementation of any V2V approach, access to the on-board instrumentation sensors and BMS controllers of the provider and receiver EVs are required to establish a communication between two EVs and to fetch the required parameters for V2V. These aspects of V2V are already discussed in [10]–[12], with details of game theory-based algorithms to match the receiver and the provider EVs with an assumption that the bidirectional power converter interface for V2V is available. Practical implementation of the proposed V2V approach for commercial EVs assumes that communication between EVs and access to controllers and instrumentation sensors is readily available as detailed in [10]–[12] and proposes to provide a powerful interface for the actual V2V power transfer through the on-board type-2 charger's hardware components. The provider EV and the receiver EV are connected directly through the existing on-board type-2 charging ports for V2V energy sharing. Depending on the battery voltage levels, provider, and receiver preferences, fetched using the on-board instrumentation sensors and EV user inputs, the V2V mode is decided, as shown in Fig. 6. Based on the mode of operation selected (e.g., forward boost), the power flow direction and the required amount of energy transfer are commanded through the on-board DSP controllers. Active rectifiers of both the on-board chargers are controlled to act as an interface by turning on the top and bottom switches of any two legs. Once the dc-links of both the on-board chargers are connected, depending on the selected V2V mode the battery side dc–dc converter of the on-board chargers is current-controlled, to deliver the

TABLE I
SIMULATION PARAMETERS OF THE PROPOSED V2V APPROACH

Parameter	**Value**
Battery-1 capacity (E_{bat1})	40 kWh
Battery-2 capacity (E_{bat2})	100 kWh
Battery-1 nominal voltage (V_{bat1})	350 V
Battery-2 nominal voltage (V_{bat2})	450 V
Switching frequency (f_{sw})	20 kHz
Filter inductor (L_1)	0.5 mH
Filter inductor (L_2)	0.6 mH
L_1 Internal resistance (R_1)	0.005 Ω
L_2 Internal resistance (R_2)	0.006 Ω
DC-link capacitor (C_1)	1000 uF
DC-link capacitor (C_2)	1100 uF
DC-DC converter-1 capacitor (C_{b1})	5.6 nF
DC-DC converter-2 capacitor (C_{b2})	5.8 nF

required charge to the receiver EV as discussed in the initial parts of this section.

IV. SIMULATION RESULTS

The proposed V2V approach is validated through MATLAB/Simulink simulation study for the forward boost and reverse buck mode with $V_{\text{bat1}} < V_{\text{bat2}}$ and $V_{\text{bat1}} = V_{\text{bat2}}$. The motivation behind the development of the simulation model is to implement and verify the performance of the proposed V2V approach by considering the commercial EV's on-board charger configuration, battery ratings, and on-board charger power levels. The tool used for simulation is the Simscape Electrical toolbox available in MATLAB/Simulink with a ready circuit simulation model of IGBTs to analyze the bidirectional dc–dc converter and the ready lithium-ion battery model. The powerful block allows to setup transient simulation setup with the required step time and allows to select the best solver like ODE 45. The simulation parameters considered for designing the EV-1 and EV-2 on-board chargers are given in Table I. The simulation results for reverse boost and forward buck mode $V_{\text{bat1}} > V_{\text{bat2}}$ and $V_{\text{bat1}} = V_{\text{bat2}}$ are similar to the forward boost and reverse buck mode with $V_{\text{bat1}} < V_{\text{bat2}}$ and $V_{\text{bat1}} = V_{\text{bat2}}$, respectively.

A. Forward Boost Mode ($V_{bat1} < V_{bat2}$)

In this mode, the energy is transferred from EV-1 battery to EV-2 battery by controlling the inductor current I_{L1}. The reference inductor current I_L^* for the forward boost mode is initially kept as 30 A and gradually increased in steps of 10 A up to 50 A to control the EV-1 battery discharge current I_{b1}. The control of I_{b1} and the corresponding drop in state of charge (SOC) of EV-1 SoC_{b1}, voltage V_{b1}, and the discharged power out of EV-1 battery P_{b1} is shown in Fig. 8(a). EV-2 battery charging current I_{b2} and the corresponding rise in SoC_{b2}, V_{b2}, and charged power of EV-2 battery P_{b2} are shown in Fig. 8(b). A positive value of battery current represents discharging and a negative value represents the charging of the battery. Discharging and charging currents are within the current rating of the active rectifier switches I_{s1r} which is 45 A for the on-board type-2 charger.

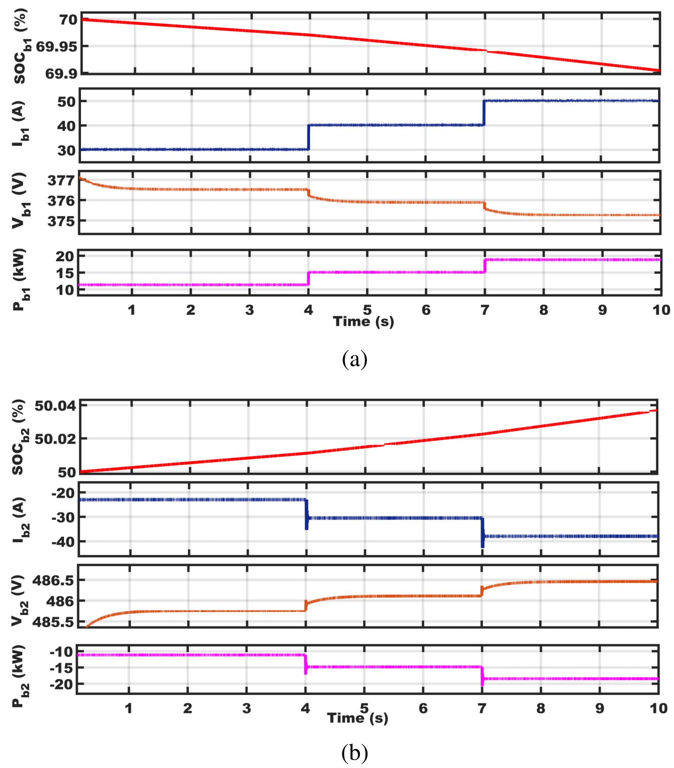

Fig. 8. Simulation results of the proposed V2V operation in forward boost mode with $V_{\text{bat1}} < V_{\text{bat2}}$. (a) SOC, voltage, current, and power waveforms of EV-1 battery. (b) SOC, voltage, current, and power waveforms of EV-2 battery.

B. Reverse Buck Mode ($V_{bat1} < V_{bat2}$)

In this mode, for the same EV-1 and EV-2 battery voltage levels as the forward boost mode but the power flow is reversed. The receiver EV-1 battery is charged with the charging current I_{b1} and the corresponding rise in SOC and voltage with the charging power level is shown in Fig. 9(a). The discharging current of the EV-2 battery I_{b2} and the corresponding SOC and voltage with the EV-2 battery discharge power are shown in Fig. 9(b).

C. Forward Boost Mode ($V_{bat1} = V_{bat2}$)

This mode represents the energy transfer between two same model EVs with equal voltage cases. The currents I_{L1} and I_{L2} are controlled with the same current reference in the forward direction. Fig. 10(a) shows the discharging current of the EV-1 battery and the corresponding changes in SOC, voltage, and power. The charging current and respective changes in EV-2 battery SOC and voltage with variations in the dc-link voltages are shown in Fig. 10(b). Depending on the current reference value of the dc–dc converter-2, the dc-link voltage will be slightly higher than the EV-2 battery voltage.

D. Performance Analysis

In this section, the efficiency of the proposed V2V approach and loss calculations at different output power levels are

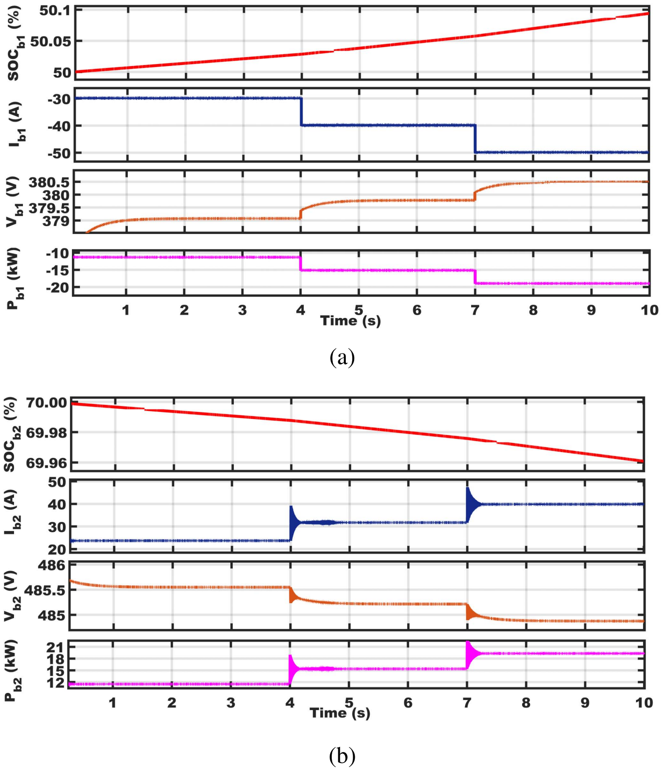

Fig. 9. Simulation results of the proposed V2V operation in the reverse buck mode with $V_{\text{bat1}} < V_{\text{bat2}}$. (a) SOC, voltage, current, and power waveforms of the EV-1 battery. (b) SOC, voltage, current, and power waveforms of the EV-2 battery.

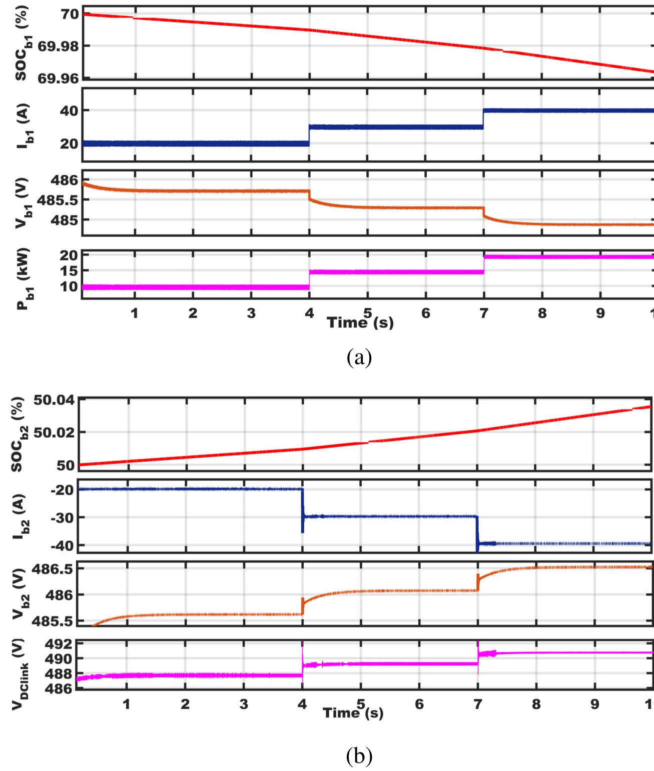

Fig. 10. Simulation results of the proposed V2V operation in the forward boost mode with $V_{\text{bat1}} = V_{\text{bat2}}$. (a) SOC, voltage, current, and power waveforms of EV-1 battery. (b) SOC, voltage, current of EV-2 battery, and dc-link voltage.

presented. The main losses incurred during V2V power transfer operation are switching and conduction losses of the on-board charger's switches and the ohmic losses in filter inductors. The switching and conduction losses calculations of the diode and the IGBTs are calculated based on the basic equations given in [21].

The power losses and power conversion efficiency in the forward boost mode for the reference inductor current I_L^* of 30 A are presented in Table II. There is no switching loss in dc–dc converter-2 since S_{a2} is kept ON and S_{b2} is kept OFF throughout this mode. The power conversion efficiency and power losses due to switching and conduction with respect to the output power are shown in Fig. 11. The V2V efficiency and losses are computed for three different output power levels P_{output} which are ≈11, ≈14, and ≈18 kW according to the change in reference inductor current I_L^* as shown in Fig. 8(b). As I_L^* increases, the corresponding power losses also increase due to higher energy transfer between two EVs and thus, the power conversion efficiency (η) decreases with higher output power. The conduction losses in inductors L_1 and L_2 are relatively low due to low value of internal resistances R_1 and R_2.

Furthermore, to show the improved performance of the proposed V2V approach, it is quantitatively compared with a similar V2V approach presented in [18] as shown in Table III. The proposed V2V approach connects the two EVs through the type-2 three-phase on-board chargers of 19.4 kW rated power. The V2V approach presented in [18] utilizes type-1

TABLE II
POWER LOSSES FOR THE PROPOSED V2V OPERATION IN THE FORWARD BOOST MODE

Parameter	Value
DC-DC converter-1 switching losses ($P_{SW,DC1}$)	132 W
DC-DC converter-1 conduction losses ($P_{cond,DC1}$)	14.1 W
Type-2 active rectifier-1 conduction losses ($P_{cond,AR1}$)	9.6 W
DC-DC converter-2 switching losses ($P_{SW,DC2}$)	0 W
DC-DC converter-2 conduction losses ($P_{cond,DC2}$)	12.77 W
Type-2 active rectifier-2 conduction losses ($P_{cond,AR2}$)	9.6 W
Input power (P_{input})	11.35 kW
Output power (P_{output})	11.172 kW
Power conversion efficiency (η)	98.43 %

single-phase on-board chargers with maximum power limited to 3.3 kW. In [18], V2V power transfer is carried out using four stages (dc to dc, dc to ac, ac to dc, and then back dc–dc). For an adequate comparison, the approach presented in [18] is carried out for 19.4 kW three-phase system and quantitatively compared with the proposed V2V approach. The proposed approach with fewer conversion stages and less number of

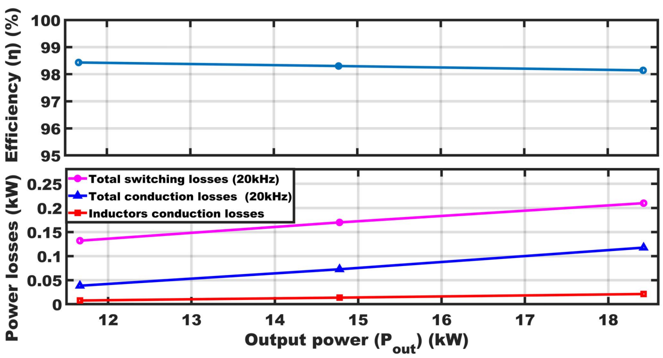

Fig. 11. Efficiency and power losses versus output power.

TABLE III
COMPARISON BETWEEN THE PROPOSED AND PRESENTED V2V APPROACH IN [18]

Parameter	**Proposed**	**[18]**
Power conversion stages	2	4
Total conduction losses	0.203 kW	0.56 kW
Total switching losses	0.2 kW	2.284 kW
Switching frequency (f_{sw})	20 kHz	20 kHz
Efficiency (η)	97.92 %	85.34 %
Battery voltage (V_{bat})	450 V	450 V
Battery capacity (E_{bat})	100 kWh	100 kWh
Maximum possible battery charging current (I_{bat})	45 A	45 A
Total charging time for 20 % charging	1 Hr	1 Hr
On-board type-2 charger power rating	19.4 kW	19.4 kW

active switches have lower total switching loss (0.2 kW) and conduction loss (0.203 kW). The V2V approach in [18] having four conversion stages results in higher switching loss (2.28 kW) and conduction loss (0.56 kW). Lower losses in the case of the proposed V2V approach result in the improved efficiency of 97.92% compared to the 85.34% efficiency of the multistage conversion-based V2V approach presented in [18]. With respect to the charging time, the proposed approach and the three-phase equivalent of the V2V approach presented in [18] are equal and take nearly 1 h to rise the SOC of the EV battery by 20% with a nominal voltage of 450 V and 100 kWh capacity.

Due to the limited power rating of the on-board chargers, the type-2 on-board charger power ranges around 19.4 kW limiting the overall charging time to 4–6 h for fully charging the battery. As the proposed V2V approach utilizes type-2 on-board chargers, the same charging time limitation applies to the proposed approach also. However, the main idea of the V2V approach is to charge the receiver EV battery as an emergency option (e.g., charging in the range of 10%–20% of the full charge SOC) which should take less than an hour such that the receiver EV reaches the nearest charging point. Thus, the higher charging time limitation of the type-2 on-board charger is not a concern for the proposed V2V approach.

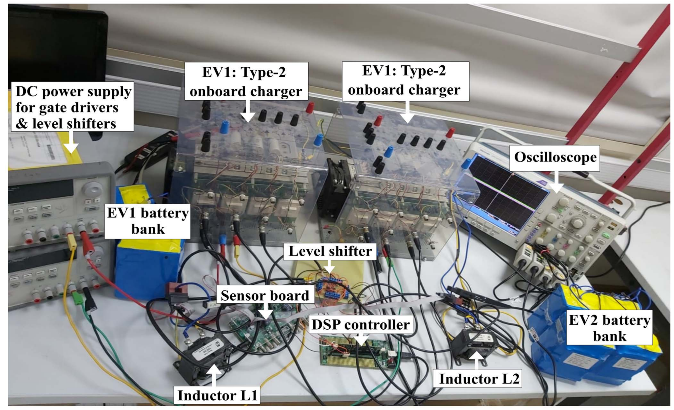

Fig. 12. Experimental setup for energy transfer between two sets of battery banks.

TABLE IV
EXPERIMENTAL PARAMETERS OF THE PROPOSED V2V APPROACH

Parameter	**Value**
Battery-1 nominal voltage (V_{bat1})	120 V
Battery-2 nominal voltage (V_{bat2})	240 V
Battery-1 and 2 nominal capacity (Ah)	5 Ah
Switching frequency (f_{sw})	20 kHz
Filter inductors (L_1&L_2)	1 mH
DC-link capacitors (C_1 & C_2)	2200 μF
DC-DC converters capacitors (C_{b1} & C_{b2})	800 μF

Reducing this V2V charging time as short as possible is critical for the widespread utilization of the V2V charging concept.

V. EXPERIMENTAL VERIFICATION

The proposed V2V approach using the on-board type-2 chargers is practically validated through the scaled 1.2 kW laboratory prototype. The complete experimental setup to transfer energy between two lithium-ion battery banks is shown in Fig. 12. The EV-1 and EV-2 on-board type-2 chargers are realized through two Semikron converter stacks each with four half-bridge IGBT legs. One of the half-bridge legs in each stack is configured as dc–dc converter and the other three half-bridge legs of each stack are configured as the active rectifier legs. The values of the battery parameters, switching frequency, and the passive components are tabulated in Table IV.

The experimental results for the proposed V2V approach are presented in Figs. 13–15. In the forward boost mode with V_{bat1}(129 V) $<$ V_{bat2}(272 V), the current through inductor L_1 is controlled in steps by varying the current reference in steps of 1.85 A to show the different operating power of the V2V charging. The EV-1 and EV-2 battery voltages and respective battery currents variation as per the reference current command are shown in Fig. 13. To maintain the same convention as simulation, I_{b2} is shown as negative to indicate the charging of the EV-2 battery and I_{b1} as positive to show discharging of the EV-1 battery.

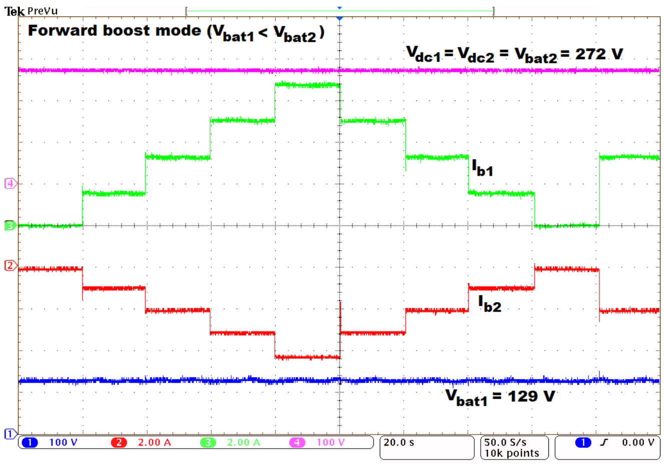

Fig. 13. Experimental results: battery voltages and currents for EV-1 and EV-2 in forward boost mode ($V_{\text{bat1}} < V_{\text{bat2}}$).

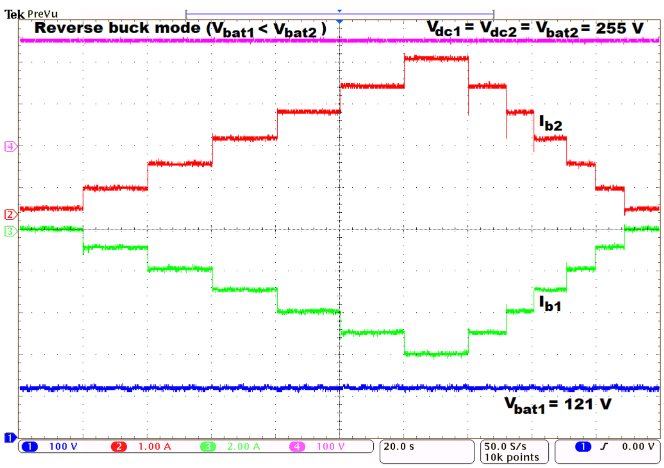

Fig. 14. Experimental results: battery voltages and currents for EV-1 and EV-2 in the reverse buck mode ($V_{\text{bat1}} < V_{\text{bat2}}$).

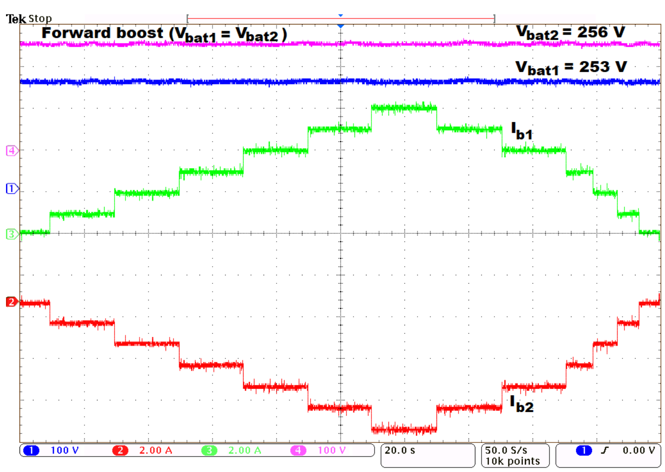

Fig. 15. Experimental results: Battery voltages and currents for EV-1 and EV-2 in forward boost mode ($V_{\text{bat1}} = V_{\text{bat2}}$).

For the reverse buck mode with nearly the same battery voltage condition $V_{\text{bat1}}(121\text{ V}) < V_{\text{bat2}}(255\text{ V})$, the results are similar to the forward boost mode with the power flow reversed. In the reverse buck mode, the EV-1 battery is charged with a negative value of I_{b1} and the EV-2 battery is discharging with a positive value of I_{b2}. The EV-1 and EV-2 battery voltages and variation of the battery currents for different V2V operating power in reverse buck mode are shown in Fig. 14.

For the V2V energy transfer in the forward boost mode with the EV-1 and EV-2 battery voltages nearly equal voltage $V_{\text{bat1}}(261\text{ V}) \approx V_{\text{bat2}}(265\text{ V})$, both the inductor currents I_{L1} and I_{L2} are controlled with the same reference with equal magnitude. The EV-1 and EV-2 battery voltages and discharging current I_{b1} and charging currents I_{b2} with equal magnitude are shown in Fig. 15. Thus, the experimental results clearly demonstrate the practical feasibility and effective V2V energy sharing through the on-board EV chargers without the need for additional hardware.

VI. Conclusion

This article proposes a direct V2V charging approach for power transfer between two EVs without the need for external hardware or additional charging ports. It is an emergency rescue charging solution in the case of non-availability of ac grid and dc fast-charging stations. Connecting two EV batteries directly through the on-board charger ports leads to significant hardware infrastructure savings. The redundant power conversion stages were avoided, which improved the overall efficiency of the proposed V2V approach which is evident in the performance analysis. The proposed V2V approach mitigates range anxiety and cooperatively shares energy between EV users with minimum infrastructure and cost. The proposed V2V method is validated through simulation in MATLAB/Simulink and experimental results which prove the practical effectiveness without modifying the EV power architecture.

References

[1] J. Yuan, L. Dorn-Gomba, A. D. Callegaro, J. Reimers, and A. Emadi, “A review of bidirectional on-board chargers for electric vehicles,” *IEEE Access*, vol. 9, pp. 51501–51518, 2021.

[2] M. Y. Metwly, M. S. Abdel-Majeed, A. S. Abdel-Khalik, R. A. Hamdy, M. S. Hamad, and S. Ahmed, “A review of integrated on-board EV battery chargers: Advanced topologies, recent developments and optimal selection of FSCW slot/pole combination,” *IEEE Access*, vol. 8, pp. 85216–85242, 2020.

[3] A. Khaligh and M. D’Antonio, “Global trends in high-power on-board chargers for electric vehicles,” *IEEE Trans. Veh. Technol.*, vol. 68, no. 4, pp. 3306–3324, Apr. 2019.

[4] V. T. Tran, D. Sutanto, and K. M. Muttaqi, “The state of the art of battery charging infrastructure for electrical vehicles: Topologies, power control strategies, and future trend,” in *Proc. Australas. Universities Power Eng. Conf. (AUPEC)*, Nov. 2017, pp. 1–6.

[5] M. R. Khalid, I. A. Khan, S. Hameed, M. S. J. Asghar, and J.-S. Ro, “A comprehensive review on structural topologies, power levels, energy storage systems, and standards for electric vehicle charging stations and their impacts on grid,” *IEEE Access*, vol. 9, pp. 128069–128094, 2021.

[6] M. Yilmaz and P. T. Krein, “Review of battery charger topologies, charging power levels, and infrastructure for plug-in electric and hybrid vehicles,” *IEEE Trans. Power Electron.*, vol. 28, no. 5, pp. 2151–2169, May 2013.

[7] G. Li, L. Boukhatem, L. Zhao, and J. Wu, “Direct vehicle-to-vehicle charging strategy in vehicular Ad-Hoc networks,” in *Proc. 9th IFIP Int. Conf. New Technol., Mobility Secur. (NTMS)*, Jan. 2018, pp. 1–5.

[8] R. Q. Zhang, X. Cheng, and L. Q. Yang, “Flexible energy management protocol for cooperative EV-to-EV charging,” *IEEE Trans. Intell. Transp. Syst.*, vol. 20, no. 1, pp. 172–184, Jan. 2019.

[9] D. M. Mughal, J. S. Kim, H. Lee, and M. Y. Chung, "Performance analysis of V2V communications: A novel scheduling assignment and data transmission scheme," *IEEE Trans. Veh. Technol.*, vol. 68, no. 7, pp. 7045–7056, Jul. 2019.

[10] E. Bulut and M. C. Kisacikoglu, "Mitigating range anxiety via vehicle-to-vehicle social charging system," in *Proc. IEEE 85th Veh. Technol. Conf. (VTC Spring)*, Jun. 2017, pp. 1–5.

[11] P. You and Z. Yang, "Efficient optimal scheduling of charging station with multiple electric vehicles via V2V," in *Proc. IEEE Int. Conf. Smart Grid Commun. (SmartGridComm)*, Nov. 2014, pp. 716–721.

[12] A.-M. Koufakis, E. S. Rigas, N. Bassiliades, and S. D. Ramchurn, "Towards an optimal EV charging scheduling scheme with V2G and V2V energy transfer," in *Proc. IEEE Int. Conf. Smart Grid Commun. (SmartGridComm)*, Nov. 2016, pp. 302–307.

[13] E. Ucer *et al.*, "A flexible V2V charger as a new layer of vehicle-grid integration framework," in *Proc. IEEE Transp. Electrific. Conf. Expo (ITEC)*, Jun. 2019, pp. 1–7.

[14] C. Liu, K. T. Chau, D. Wu, and S. Gao, "Opportunities and challenges of vehicle-to-home, vehicle-to-vehicle, and vehicle-to-grid technologies," *Proc. IEEE*, vol. 101, no. 11, pp. 2409–2427, Nov. 2013.

[15] P. Mahure, R. K. Keshri, R. Abhyankar, and G. Buja, "Bidirectional conductive charging of electric vehicles for V2V energy exchange," in *Proc. 46th Annu. Conf. IEEE Ind. Electron. Soc. (IECON)*, Oct. 2020, pp. 2011–2016.

[16] *Andromeda Power*. Accessed: Nov. 2021. [Online]. Available: https://www.andromedapower.com

[17] Dec. 2019. *Hyundai introduces vehicle to vehicle charging facility*. Accessed: Nov. 2021. [Online]. Available: https://www.autocarindia.com/car-news/hyundai-introduces-vehicle-to-vehicle-charging-facility-415144

[18] S. Taghizadeh, M. J. Hossain, N. Poursafar, J. Lu, and G. Konstantinou, "A multifunctional single-phase EV on-board charger with a new V2V charging assistance capability," *IEEE Access*, vol. 8, pp. 116812–116823, 2020.

[19] T. J. C. Sousa, V. Monteiro, J. C. A. Fernandes, C. Couto, A. A. N. Meléndez, and J. L. Afonso, "New perspectives for vehicle-to-vehicle (V2V) power transfer," in *Proc. 44th Annu. Conf. IEEE Ind. Electron. Soc.*, Oct. 2018, pp. 5183–5188.

[20] R. W. Erickson and D. Maksimovic, *Fundamentals of Power Electronics*, 2nd ed. Norwell, MA, USA: Springer, 2007.

[21] D. Graovac and M. Purschel, "IGBT power losses calculation using the data-sheet parameters-application note," Infineon Technol. AG, Neubiberg, Germany, Appl. Note V 1.1, Jan. 2009.

Azizulrahman Shafiqurrahman (Student Member, IEEE) received the B.Sc. degree in electrical and electronics engineering from the University of Sharjah, Sharjah, United Arab Emirates, in 2020. He is currently pursuing the M.Sc. degree in electrical and computer engineering with the Department of Electrical Engineering and Computer Science, Khalifa University, Abu Dhabi, United Arab Emirates.

His current research interests include power electronics applications, energy conversion in electrified transportation, and vehicle-to-vehicle charging.

B. S. Umesh (Member, IEEE) received the B.E. degree in electrical and electronics engineering from the University B. D. T. College of Engineering, Davanagere, India, in 2007, the M.Tech. degree in power electronics and drives from the National Institute of Technology Warangal, Warangal, India, in 2011, and the Ph.D. degree in electrical engineering from the Indian Institute of Technology Hyderabad (IITH), Hyderabad, India, in 2016.

He was a Research Consultant at GE Global Research, Bengaluru, India, in 2017, and a Lead Engineer at GE Aviation, Bengaluru, in 2019. He is currently a Post-Doctoral Fellow with the Department of Electrical Engineering and Computer Science, Khalifa University, Abu Dhabi, United Arab Emirates. His research interests include power converter design and development for electric vehicle charging, more electric aircraft, multi-phase induction motor drives, and pole-phase modulation of induction motor drives.

Naji Al Sayari (Member, IEEE) received the B.Sc. degree in electrical engineering from the Florida Institute of Technology, Melbourne, FL, USA, in 2001, the M.Sc. degree in electrical engineering from Washington University in St. Louis, St. Louis, MO, USA, in 2005, and the Ph.D. degree from The University of Manchester, Manchester, U.K., in 2011.

He is currently an Associate Professor with the Department of Electrical Engineering and Computer Science, Khalifa University, Abu Dhabi, United Arab Emirates. He is also the Co-Founder of the Power Electronics and Advanced Sustainable Energy (PEACE) Laboratory, Khalifa University. His current research interests include electric machine analysis, power electronics applications, power quality issues, distributed generation, smart grid, micro-grid, and renewable energy systems.

Vinod Khadkikar (Fellow, IEEE) received the M.Tech. degree in power electronics, electrical machines, and drives from the Indian Institute of Technology Delhi (IITD), New Delhi, India, in 2002, and the Ph.D. degree in electrical engineering from the École de Technologie Supérieure, Montreal, QC, Canada, in 2008.

From December 2008 to March 2010, he was a Post-Doctoral Fellow with the University of Western Ontario, London, ON, Canada. In 2010, he was a Visiting Professor with the Massachusetts Institute of Technology (MIT), Cambridge, MA, USA. He is currently a Professor with the Department of Electrical Engineering and Computer Science, Khalifa University, Abu Dhabi, United Arab Emirates. His research interests include the applications of power electronics in distribution systems and renewable energy resources, grid interconnection issues, power quality enhancement, active power filters, and electric vehicles.

Dr. Khadkikar is currently an Associate Editor for the IEEE TRANSACTIONS ON INDUSTRIAL ELECTRONICS, IEEE TRANSACTIONS ON INDUSTRY APPLICATIONS, and *IET Power Electronics*. He is a Distinguished Lecturer of the IEEE Industry Applications Society.